Strong Dependence of Quantum-Dot Delayed Luminescence on Excitation Pulse Width

Arianna Marchioro,[§,‡] Patrick J. Whitham,[‡] Heidi D. Nelson,[‡] Michael C. De Siena, Kathryn E. Knowles,[†] Victor Z. Polinger, Philip J. Reid, and Daniel R. Gamelin[*]

Department of Chemistry, University of Washington, Seattle, Washington 98195-1700, United States

Abstract. Delayed luminescence involving charge-carrier trapping and detrapping has recently been identified as a widespread and possibly universal phenomenon in colloidal quantum dots. Its near-power-law decay suggests a relationship with blinking. Here, using colloidal $CuInS_2$ and CdSe quantum dots as model systems, we show that short (ns) excitation pulses yield less delayed luminescence intensity and faster delayed luminescence decay than observed with long (ms) square-wave excitation pulses. Increasing the excitation power also affects the delayed luminescence intensity, but the delayed luminescence decay kinetics appear much less sensitive to excitation power than to excitation pulse width. An idealized four-state kinetic model reproduces the major experimental trends and highlights the very slow approach to steady state during photoexcitation, stemming from extremely slow detrapping of the metastable charge-separated state responsible for delayed luminescence. The impacts of these findings on proposed relationships between delayed luminescence and blinking are discussed.

TOC Graphic

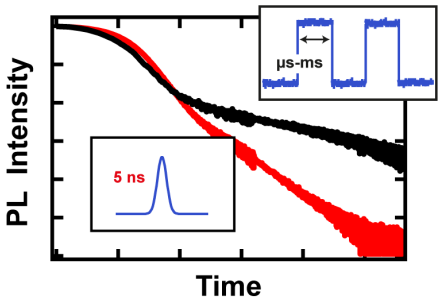

Several groups have reported extremely slow photoluminescence decay in various colloidal semiconductor nanostructures, including CdSe[1-5] and copper-doped CdSe (Cu^+:CdSe)[3,5] quantum dots, CdSe nanoplatelets,[6] lead-halide perovskite nanocrystals,[7] and $CuInS_2$ quantum dots,[5,8] persisting for times that vastly exceed the natural excited-state lifetimes of these materials. In each case, the delayed luminescence shows broadly distributed decay kinetics with components ranging from sub-microsecond to beyond seconds. This delayed luminescence is explained by invoking temporary charge-carrier trapping at a quantum dot surface, followed by spontaneous detrapping to re-form the emissive core state. Detrapping occurs *via* tunneling.[5-6] This delayed luminescence has been related to the photoluminescence blinking of single quantum dots.[1,3-5,8-9] A better understanding of the carrier trapping and detrapping processes responsible for delayed luminescence would provide insight into the characteristics of surface traps to help guide optimization of the photophysical properties of colloidal semiconductor quantum dots.

We recently reported that the ratio of delayed to prompt luminescence intensities depends strongly on the quantum dot photoexcitation rate,[8] because the delayed luminescence saturates at excitation rates that are orders of magnitude smaller than required to saturate the prompt luminescence of the same quantum dot. This explanation invokes efficient non-radiative recombination (*e.g.*, Auger, Shockley-Read-Hall) upon photoexcitation of a quantum dot that is already in a metastable charge-separated excited state, as also invoked to explain the low photoluminescence quantum yields of blinking "off" states.[10-12] Here, using two model nanocrystals ($CuInS_2$ and CdSe quantum dots, see Supporting Information for details), we report that even at fixed photoexcitation rates, the ratio of delayed to prompt luminescence intensities changes as the excitation pulse width is increased from nanoseconds to milliseconds. This result

is illustrated using an idealized four-state kinetic model that accounts for trapping, detrapping, and recombination processes. Additionally, we find that even the *kinetics* of the delayed luminescence are influenced by the photoexcitation pulse width, with increasing pulse widths yielding slower delayed-luminescence decay. These effects have not been observed previously.

To illustrate the central new observation reported here, Figure 1 plots two photoluminescence decay curves measured for the same d = 3.9 nm $CuInS_2$ quantum dot sample using two different common photoexcitation conditions, both with the same excitation wavelength (405 nm). In one, a 5 ns excitation pulse was used, and in the other a 100 ms square pulse was used. Both curves show prompt decay on the microsecond timescale (τ_{prompt} = 2 μs) followed by delayed luminescence extending to milliseconds and beyond. Strikingly, the two delayed luminescence decay curves have very different slopes in this log-log plot (1.11 for the 5 ns pulse vs 0.48 for the 100 ms pulse, between 50 μs and 2 ms). The delayed luminescence generated using ns pulses has decayed almost completely within ~50 ms, whereas that generated using 100 ms pulses is much longer-lived, being >100 times more intense than the former after 10 ms. The slopes of such log-log delayed luminescence plots have been related to blinking power-law exponents,[1,4,9] but the data in Figure 1 demonstrate that these slopes are dramatically influenced by the photoexcitation pulse profile itself, an observation that has not been noted previously. It is important to identify the source of the difference in decay dynamics shown in Figure 1.

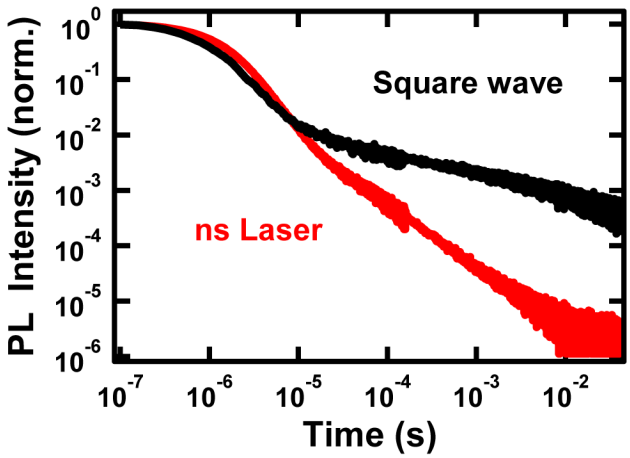

Figure 1. Photoluminescence decay curves measured for the same d = 3.9 nm $CuInS_2$ quantum dots using the same photoexcitation wavelength (405 nm) but different types of common excitation pulses. Black: 100 ms square-wave excitation pulse, 8 mW/cm^2 pulse power, 5 Hz repetition rate. Red: 5 ns excitation pulse, 30 μJ/cm^2, 20 Hz repetition rate. These data show that delayed luminescence decay dynamics depend on photoexcitation conditions. Data are normalized using the peak prompt luminescence intensity for the 5 ns pulse data and the luminescence intensity during excitation for the 100 ms pulse data. For these and all other data in this manuscript, t = 0 coincides with the end of the square-wave pulse. All data collected at 20 K.

We hypothesized that two major experimental parameters might contribute to the differences observed in Figure 1: the excitation power and its duration. To test the roles of these two parameters, variable-pulse-width photoexcitation experiments were performed at different laser powers. Because the delayed luminescence decay dynamics are temperature-independent over a very broad range,[5-6] all data reported here were collected at 20 K to minimize thermally activated nonradiative decay[5] and irreversible photodegradation. Figure 2 summarizes the effects of photoexcitation pulse duration and power on the delayed luminescence decay dynamics of the same $CuInS_2$ quantum dots. Figure 2A plots the $CuInS_2$ quantum dot delayed-luminescence decay dynamics (normalized to the prompt-luminescence intensity, which is independent of pulse duration under these conditions) as a function of excitation pulse duration from 50 μs to 100 ms. Except for a small amount of irreversible photodegradation over these very long measurements (*e.g.*, <~10% over ~20 hours of continuous measurement for the data in Figure

2A), the prompt-luminescence intensity is linearly proportional to the photoexcitation power.[8] As the pulse width increases, the delayed luminescence intensity grows and the slopes of the delayed luminescence decay curves in the log-log plot decrease. We interpret this result as indicating that accumulation of population in the metastable charge-separated excited state is very slow, and hence very long excitation pulses are required to reach steady state.

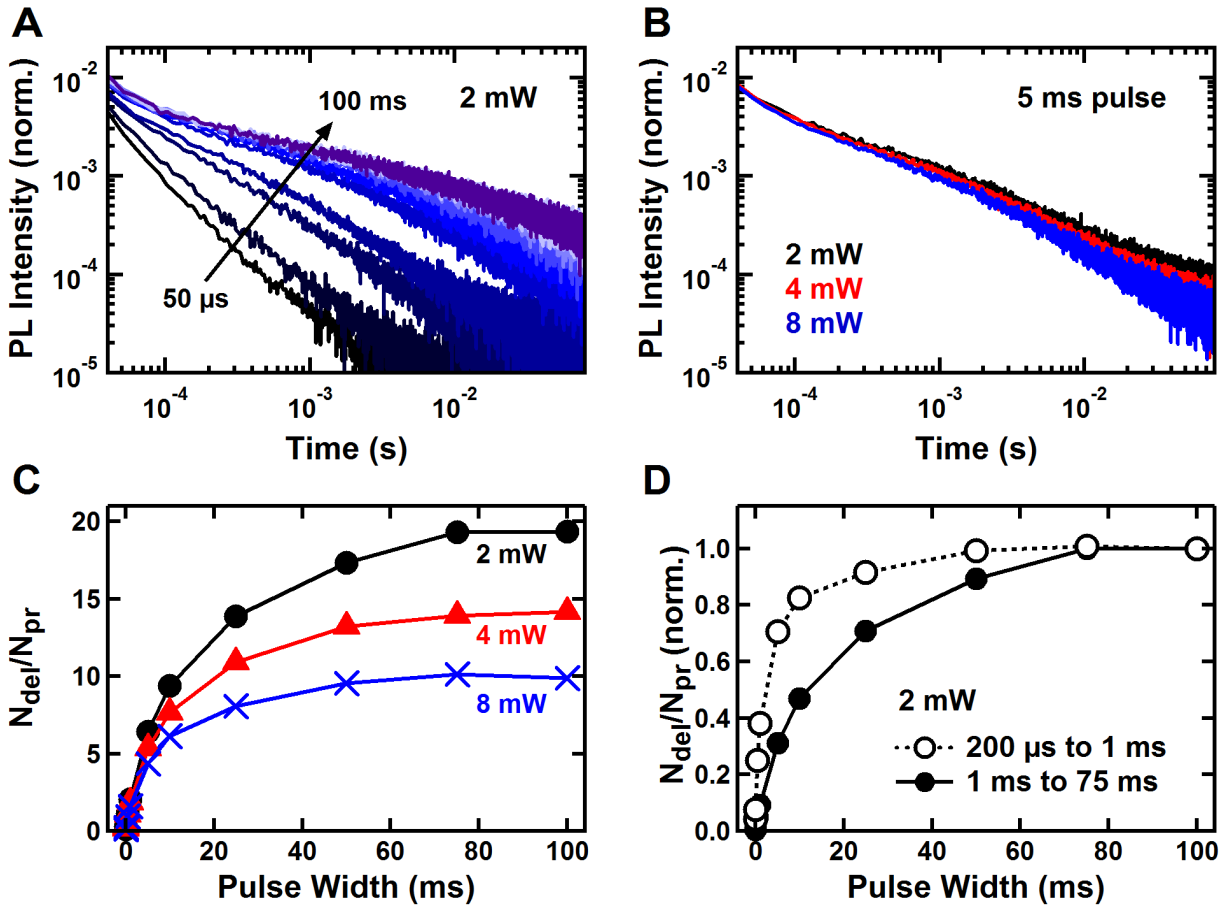

Figure 2. (A) Dynamics of delayed luminescence for increasing pulse width for d = 3.9 nm $CuInS_2$ quantum dots (50 µs (black) to 100 ms (purple) excitation pulse width). Traces are normalized to the prompt luminescence intensity. **(B)** Dynamics of delayed luminescence measured using 2 (black), 4 (red), and 8 mW (blue) excitation powers (power densities = 6.7, 13.3, and 26.7 mW/cm^2) for the same $CuInS_2$ quantum dots, with a 5 ms excitation pulse. Traces are normalized to the prompt luminescence intensity. Linear plots of the data in (A) and (B) are provided as Supporting Information. **(C)** N_{del}/N_{pr} calculated from decay curves such as those in (A) and (B) for the same $CuInS_2$ quantum dots, plotted *vs* excitation pulse width and measured at three different excitation powers: 2 mW (black circles), 4 mW (red triangles), 8 mW (blue crosses). **(D)** Values of

N_{del}/N_{pr} for the same $CuInS_2$ quantum dots, collected at 2 mW, plotted *vs* excitation pulse width, and normalized to the value of N_{del}/N_{pr} at 100 ms pulse width. Two delayed luminescence integration windows are represented: a shorter window (open circles, t_1 = 200 μs, t_2 = 1 ms) and a longer window (filled circles, t_1 = 1 ms, t_2 = 75 ms). These specific integration windows were chosen to reflect the broadest overall timespan in which signal-to-noise was good, but the same trends are obtained using different integration windows. All data collected at 20 K.

Figure 2B plots delayed luminescence decay curves measured for these same $CuInS_2$ quantum dots using fixed excitation pulse widths but excitation powers of 2, 4, and 8 mW (power densities = 6.7, 13.3, and 26.7 mW/cm^2), again normalized to the prompt luminescence intensities. The decay dynamics measured at these different excitation powers are almost indistinguishable when the pulse width is kept constant. Together, the data in Figures 2A,B demonstrate that quantum dot delayed luminescence decay *dynamics* are quite sensitive to the excitation pulse duration but are relatively insensitive to its peak power. The same conclusion holds when comparing data representing similar increases in the total number of photons per excitation pulse generated *via* an increased pulse width or excitation power. For example, the power-law slope at ~1 ms decreases from 1.15 to 0.68 upon increasing the pulse width from 100 to 500 μs at fixed 2 mW excitation power, but it remains nearly unchanged (1.23) upon increasing the excitation power from 2 to 8 mW for a fixed 100 μs pulse width (see Supporting Information).

To quantify the trends of Figures 2A,B, Figures 2C,D plot the number of delayed luminescence photons (N_{del}) normalized by the number of prompt luminescence photons (N_{pr}) for each experiment from Figures 2A,B. N_{del} is obtained by integrating delayed-luminescence decay curves such as those in Figures 2A,B over a specified time range (t_1 to t_2, eq 1), while N_{pr} is obtained by integrating the prompt luminescence up to a specified cutoff time (t_f, eq 2).

$$N_{del} = \int_{t_1}^{t_2} I(t)dt \quad (1)$$

$$N_{pr} = \int_{0}^{t_f} I_0 e^{-k_{PL}t} dt \quad (2)$$

Here, I(t) is the time-dependent luminescence intensity as seen in Figures 2A,B, I_0 is the steady-state luminescence intensity measured when the excitation pulse is on, and k_{PL} is the experimental prompt-luminescence decay constant measured by single-photon counting. For the $CuInS_2$ quantum dots, $k_{PL} = 1/\tau_{prompt} = 5 \cdot 10^5$ s^{-1} from a single-exponential fit, t_1 and t_2 correspond to 200 μs and 75 ms, respectively, and t_f corresponds to 10 μs (= $5\tau_{prompt}$). Figure 2C shows that for fixed excitation power, N_{del}/N_{pr} increases with increasing pulse width before eventually reaching a plateau value, while N_{pr} is independent of pulse width under these conditions. The ratio of delayed to prompt luminescence photons is thus pulse-width dependent, first growing with increasing excitation pulse width before plateauing at excitation pulse widths of almost 100 ms. The plateau of N_{del}/N_{pr} suggests that only with such extremely long excitation pulses does the population of the charge-separated state responsible for delayed luminescence reach steady state under photoexcitation.

For any given excitation pulse width, N_{del}/N_{pr} also decreases with increasing excitation power. This trend stems from the fact that N_{pr} increases linearly with excitation power in the investigated power range, whereas N_{del} shows a sub-linear power dependence.[8] When normalized, it is evident that the curvatures of the data in Figure 2C are essentially independent of excitation power (see Supporting Information).

Figure 2D compares experimental N_{del}/N_{pr} values obtained by integrating over two different delayed luminescence time windows (*i.e.*, different t_1 and t_2 in eq 1) for these $CuInS_2$ quantum dots. For ease of comparison, each N_{del}/N_{pr} curve is normalized to the value obtained using a pulse width of 100 ms. From these data, the delayed luminescence probed at earlier times plateaus at shorter excitation pulse widths than that collected at later times. This observation reflects the impact of the excitation pulse width on the *distribution* of delayed luminescence decay dynamics, as illustrated in Figure 1. Faster delayed luminescence can be generated from shorter excitation pulses, while slower delayed luminescence requires longer excitation pulses to reach its steady-state intensity.

To test the generality of the trends observed in Figure 2, analogous measurements were also performed on d = 3.3 nm CdSe quantum dots. Figure 3A plots delayed luminescence decay data for these quantum dots collected using 50 μs and 25 ms pulses. In this case, the change in decay dynamics is less pronounced in the range of pulse widths explored than observed in Figure 2A, but it is still significant. Figure 3B plots delayed luminescence decay curves measured at various excitation powers. As in Figure 2B, the decay dynamics change very little across this series. Figures 3C,D plot N_{del}/N_{pr} for each experiment from Figures 3A,B. k_{PL} is taken as $5 \cdot 10^8$ s^{-1} for the CdSe quantum dots; their decay is actually multi-exponential with components of ~$5 \cdot 10^8$ s^{-1} and ~$6.3 \cdot 10^7$ s^{-1}, but this distinction does not qualitatively alter the results. t_1 and t_2 correspond to 200 ns and 500 μs, and t_f corresponds to 40 ns (= ~2.5-20τ_{prompt}). Very similar trends are observed for the CdSe quantum dots (Figures 3C,D) as were observed with the $CuInS_2$ quantum dots, including the very slow (ms) approach to plateau values of N_{del}/N_{pr} with increasing pulse width (Figure 3C), the power dependence of the plateau values of N_{del}/N_{pr} but not of their curvature with increasing pulse width (Figure 3C, see also Supporting Information),

and the dependence of the curvature on the luminescence monitoring window (Figure 3D). N_{del}/N_{pr} does plateau at much longer excitation pulse widths for the $CuInS_2$ quantum dots (~80 ms, Figure 2C) than for the CdSe quantum dots (~5 ms, Figure 3C), reflecting the slower prompt luminescence of the $CuInS_2$ quantum dots and the competition between prompt luminescence and charge trapping,[5] as well as differences in the trapping/detrapping rates and experimental measurement windows (*vide infra*). Overall, the general qualitative trends are very similar for the $CuInS_2$ and CdSe quantum dots.

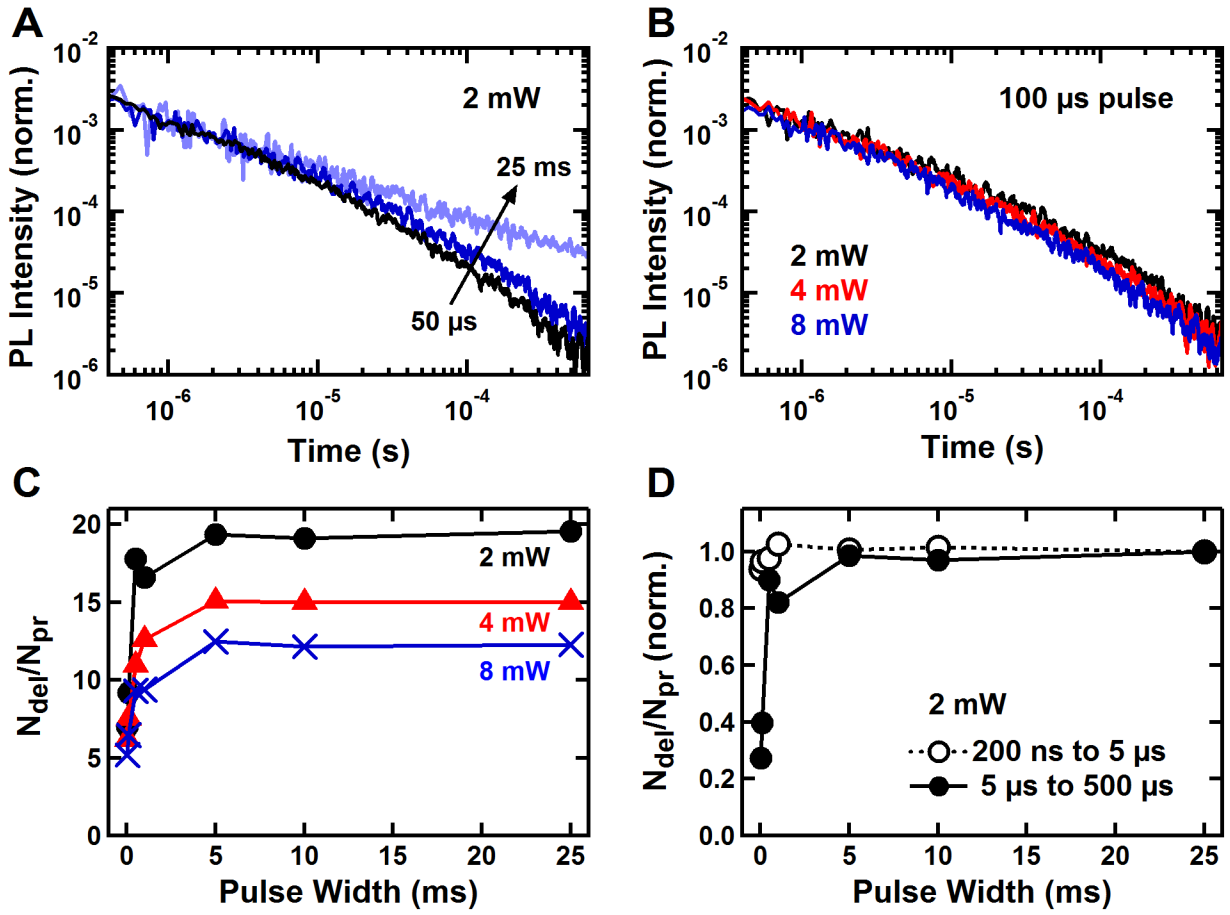

Figure 3. (A) Dynamics of delayed luminescence for increasing pulse width for d = 3.3 nm CdSe quantum dots (50 µs, 100 µs, and 25 ms excitation pulse width). Traces are normalized to the prompt luminescence intensity. **(B)** Dynamics of delayed luminescence measured using 2 (black), 4 (red), and 8 mW (blue) excitation powers (power densities = 6.7, 13.3, and 26.7 mW/cm^2) for the same CdSe quantum dots, with a 100 µs excitation pulse. Traces are normalized to the prompt luminescence intensity. Linear plots of the

data in (A) and (B) are provided as Supporting Information. **(C)** N_{del}/N_{pr} calculated from decay curves such as those in (A) and (B) for the same CdSe quantum dots, plotted *vs* excitation pulse width and measured at three different excitation powers: 2 mW (black circles), 4 mW (red triangles), 8 mW (blue crosses). **(D)** Values of N_{del}/N_{pr} for the same CdSe quantum dots, collected at 2 mW, plotted *vs* excitation pulse width, and normalized to the value of N_{del}/N_{pr} at 25 ms pulse width. Two delayed luminescence integration windows are represented: a shorter window (open circles, t_1 = 200 ns, t_2 = 5 μs) and a longer window (filled circles, t_1 = 5 μs, t_2 = 500 μs). These specific integration windows were chosen to reflect the broadest overall timespan in which signal-to-noise was good, but the same trends are obtained using different integration windows. All data collected at 20 K.

For interpretation of these experimental results, we use the four-state kinetic model summarized in Figure 4 to explore the effects of various microscopic parameters on the excitation-pulse-width dependence of N_{del}/N_{pr}. State populations within this model are described by the coupled differential equations given in eq 3. For simplicity, we adhere to idealized homogeneous (non-distributed) rate constants for these illustrations, and we discuss implications of this idealization below.

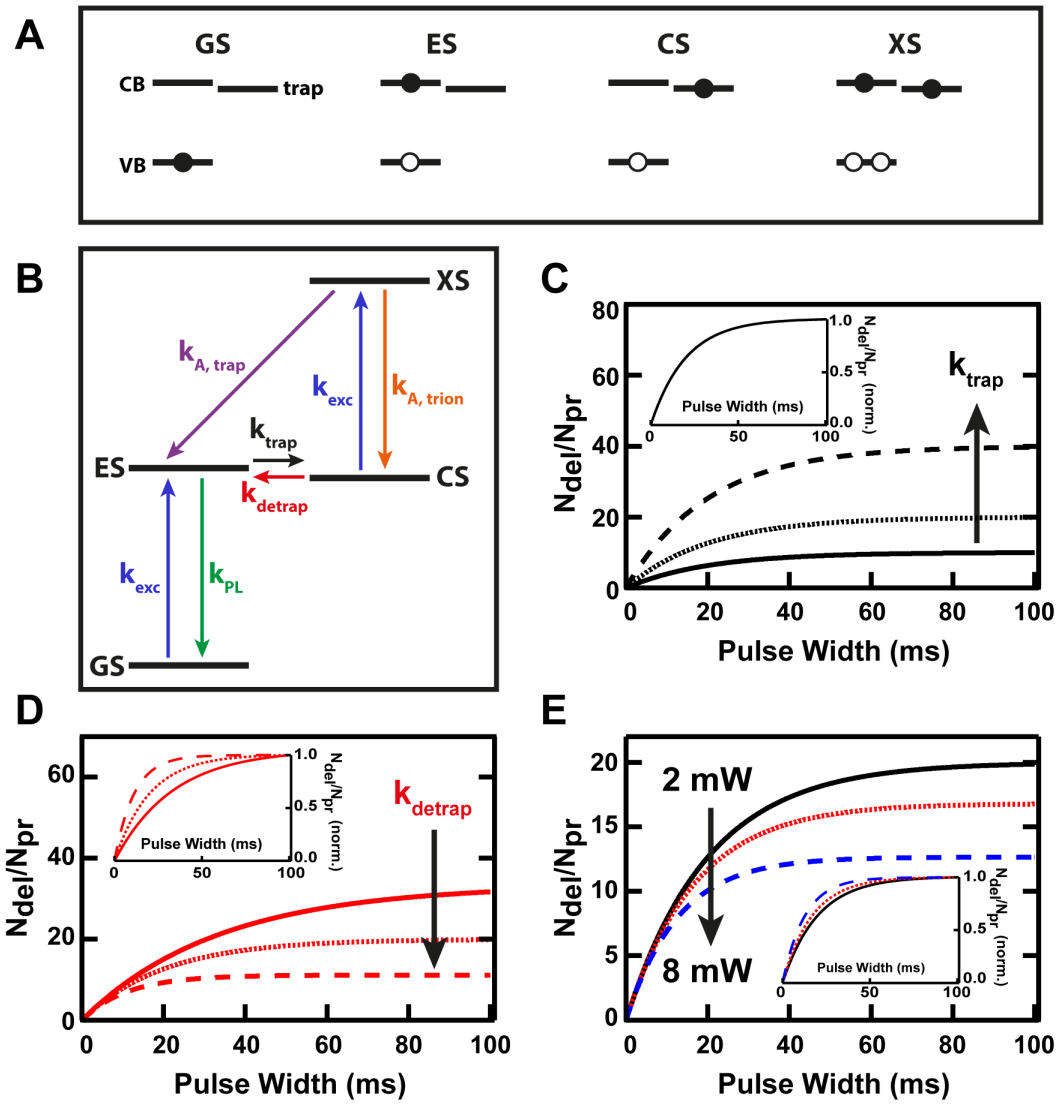

Figure 4. (A) Electronic configurations of the four states used in the model. GS = ground state, ES = excited state, CS = charge-separated state, and XS = doubly excited state. For simplicity, electron trapping is illustrated here, but the model does not depend on which specific carrier is trapped. **(B)** Four-state model used to illustrate the experimental trends. k_{exc} represents the excitation rate "constant" (with power embedded), k_{PL} is the rate constant for prompt luminescence, k_{trap} is the rate constant for formation of the metastable charge-separated state, and k_{detrap} describes detrapping from this state to reform the emissive excited state. $k_{A,trap}$ and $k_{A,trion}$ represent nonradiative trap-assisted and trion Auger processes, respectively. **(C,D)** Simulated results from this model using parameters appropriate for the $CuInS_2$ quantum dots, plotting the ratio N_{del}/N_{pr} *vs* excitation pulse width. k_{trap} and k_{detrap} are varied systematically while all the other parameters are held fixed ($k_{exc} = 20\ s^{-1}$, $k_{PL} = 5 \cdot 10^5\ s^{-1}$, $k_{A,trap} = k_{A,trion} = 10^{10}\ s^{-1}$). (C) $k_{trap} = 500\ s^{-1}$ (solid), $1000\ s^{-1}$ (dotted), $2000\ s^{-1}$ (dashed), all with $k_{detrap} = 40\ s^{-1}$. (D) $k_{detrap} = 20\ s^{-1}$ (solid), $40\ s^{-1}$ (dotted), $80\ s^{-1}$ (dashed), all with $k_{trap} = 1000\ s^{-1}$. The insets show the normalized curves for each plot. The arrows show the directions of increasing k_{trap} and k_{detrap}, respectively. **(E)** Simulated results for excitation powers of 2 ($k_{exc} = 20\ s^{-1}$, solid), 4 ($k_{exc} = 39\ s^{-1}$, dotted), and 8 mW ($k_{exc} = 78\ s^{-1}$, dashed), keeping all other parameters constant ($k_{PL} = 5 \cdot 10^5\ s^{-1}$, $k_{A,trap} = k_{A,trion} = 10^{10}\ s^{-1}$, $k_{trap} = 1000\ s^{-1}$, $k_{detrap} = 40\ s^{-1}$). The insets show the normalized curves.

$$\frac{d[GS]}{dt} = k_{\mathrm{PL}}[ES] - k_{\mathrm{exc}}[GS]$$

$$\frac{d[ES]}{dt} = k_{\mathrm{exc}}[GS] + k_{\mathrm{detrap}}[CS] + k_{\mathrm{A,trap}}[XS] - k_{\mathrm{PL}}[ES] - k_{\mathrm{trap}}[ES]$$

$$\frac{d[CS]}{dt} = k_{\mathrm{trap}}[ES] + k_{\mathrm{A,trion}}[XS] - k_{\mathrm{detrap}}[CS] - k_{\mathrm{exc}}[CS]$$

$$\frac{d[XS]}{dt} = k_{\mathrm{exc}}[CS] - k_{\mathrm{A,trap}}[XS] - k_{\mathrm{A,trion}}[XS] \quad (3)$$

Solving eq 3 yields the populations of the ground state (GS), the emissive excited state (ES), the metastable charge-separated excited state (CS), and the doubly excited state (XS) during and after excitation. Electronic configurations associated with each of these states are depicted in Figure 4A. For simplicity, we illustrate electron dynamics as rate-determining for delayed luminescence,[3] but it is likely that the hole is also localized in the metastable state;[13] the kinetic model does not rely on these specifics. In eq 3 and Figure 4B, k_{trap} and k_{detrap} describe the formation and detrapping of the metastable state and, along with k_{exc}, are the meaningful variables in these simulations. To account for the observed excitation power dependence of $N_{\mathrm{del}}/N_{\mathrm{pr}}$, the model also includes excitation from the charge-separated state to a doubly excited state, which can decay to the emissive excited state through a trap-assisted Auger process described by $k_{\mathrm{A,trap}}$ or to the charge-separated state through a trion Auger process described by $k_{\mathrm{A,trion}}$. These fast nonradiative processes are modeled with $k_{\mathrm{A,trap}} = k_{\mathrm{A,trion}} = 10^{10}$ s^{-1} for all simulations, consistent with experimentally measured rates for similar Auger processes in small NCs.[14-16]

To simulate the evolution of the state populations during the excitation pulse, eq 3 was solved with k_{exc} determined from the experimental excitation powers and extinction coefficients, and initial conditions of $[GS]_0 = 100$ and $[ES]_0 = [CS]_0 = [XS]_0 = 0$. Evaluating this result at the end of the pulse gives the populations of the states when the excitation pulse is turned off. These populations can then be used as initial conditions for solving eq 3 again with $k_{exc} = 0$ to simulate their decay with time. Simulated luminescence decay curves illustrating the effects of changing the various model parameters are included as Supporting Information.

We note that in the model calculations, all trapping and detrapping processes are much slower than the prompt luminescence (*i.e.*, k_{trap} and $k_{detrap} << k_{PL}$), so effectively, after termination of the excitation pulse the entire [ES] decays as prompt luminescence and the entire initial [CS] decays as delayed luminescence. Consequently, to a very good approximation, the values of N_{del}/N_{pr} obtained from complete integration of the model decay curves (eqs 1, 2) equal the values of [CS]/[ES] computed at the ends of the excitation pulses (see Supporting Information). The experimental systems are complicated by their distributed trapping/detrapping kinetics, because trapping/detrapping and prompt luminescence may now occur on overlapping timescales,[4] and moreover the [CS] can decay by other routes, such as *via* population of even deeper traps.[5-6] Additionally, while the model simulates only a single pulse and all excited-state populations are zero at the beginning of the pulse, ensuring complete depopulation of the charge-separated state before beginning any excitation pulse is more challenging in the laboratory because of the extremely broad distribution of detrapping kinetics and the need for signal averaging over multiple excitation pulses; delayed luminescence from these quantum dots persists even seconds after excitation,[5] albeit with very small rates.

For comparison with the experimental data in Figure 2, Figures 4C-E plot simulated values of N_{del}/N_{pr} (taken as [CS]/[ES] at the ends of the excitation pulses) as a function of excitation pulse width for various model conditions, using parameters appropriate for the $CuInS_2$ quantum dots. The simulated data in Figure 4C show that increasing k_{trap} increases the plateau magnitude of N_{del}/N_{pr}, but the inset to Figure 4C shows that the curvature of the pulse-width dependence of N_{del}/N_{pr} is only modestly influenced by k_{trap}. On the other hand, Figure 4D and its inset show that k_{detrap} influences both the plateau magnitude of N_{del}/N_{pr} and the curvature of its pulse-width dependence. From these simulations, it is thus apparent that the pulse-width dependence of N_{del}/N_{pr} is mainly dictated by k_{detrap}. In other words, the time required to reach steady state under photoexcitation is determined mainly by the slower detrapping kinetics.

Figure 4E illustrates the effect of varying the excitation pulse power, with all other parameters fixed. N_{pr} increases linearly with excitation power, whereas N_{del} saturates because of nonradiative Auger processes in the doubly excited state, resulting in a reduction of N_{del}/N_{pr} with increased excitation power at any given pulse width, as observed experimentally (Figure 2C). Notably, reproducing the experimental dependence of N_{del}/N_{pr} on excitation power requires the presence of the trap-assisted Auger pathway, although the strength of the power dependence is influenced by the ratio of $k_{A,trap}$ to $k_{A,trion}$ (see Supporting Information). This result can be understood by recognizing that of these two processes, only the trap-assisted Auger process introduces a power-dependent pathway for depopulating the charge-separated state. Trap-assisted Auger processes have been largely overlooked in nanocrystal photophysics, and only relatively recently has their significance gained recognition.[16-18] The inset to Figure 4E shows the same curves normalized to their plateau magnitudes. Again, the curvature shows very little power dependence, consistent with experiment. Overall, the model of Figure 4B and eq 3 thus

successfully reproduces the major experimental trends summarized in Figure 2C for the $CuInS_2$ quantum dots.

Although it captures the major trends, this idealized model cannot reproduce the experimental observations of Figure 2D. Specifically, this model does not capture the effect of changing the delayed luminescence integration window on the curvature of the pulse-width dependence (see Supporting Information). This discrepancy occurs because of the model's reliance on single rate constants for each microscopic process depicted in Figure 4B. The experimental observations thus allow the conclusion that the different excitation pulse-width dependence obtained when probing different delayed luminescence decay windows (Figures 2D, 3D) reflects the *distributed* kinetics of these processes. Importantly, when the experimental curves in Figures 2D and 3D are made by sampling earlier (or later) during delayed luminescence (different t_1 and t_2 in eq. 1), they selectively report on faster (or slower) subsets of dynamical processes within the distribution. These data thus point to a weak correlation between k_{trap} and k_{detrap}, both of which are broadly distributed. This insight, together with the experimental luminescence decay data in Figures 1, 2A, and 3A, therefore highlights how both the experimental excitation pulse width *and* the experimental detection window can bias the observed delayed luminescence intensities and dynamics toward a specific subset of behaviors within a broadly distributed range. These observations have important implications for any quantitative analysis of delayed luminescence amplitudes or decay dynamics.

The data presented here are in some ways reminiscent of prior observations made for CdSe/CdS core/shell quantum dots in which multi-pulse excitation with an 80 MHz repetition rate was found to yield different excitonic photoluminescence decay dynamics for few *vs* many concatenated excitation pulses.[19] This difference was analyzed in terms of an enhanced

contribution from multiply excited quantum dots when multiple excitation pulses were delivered in short succession. The approach of using rapid sequential photoexcitation with a tunable number of short pulses is analogous to our use of variable square-wave pulse-widths in the present study. Just like at high powers in ref. 19, simulation of our long-pulse decay data by addition of multiple offset short-pulse decay curves fails to reproduce the experimental long-pulse data (see Supporting Information), pointing to multi-excitation effects even at these low powers and supporting the conclusion of trap-assisted Auger recombination deduced from the data in Figures 2C and 3C. Of course, the microscopic processes described in ref. 19 occurred on much shorter timescales than those studied here. For example, steady state was reached within ~100 ns of quasi-continuous excitation in ref. 19, whereas Figure 2C shows that steady state is not reached until ~80 ms of continuous excitation for the $CuInS_2$ quantum dots (or ~5 ms for CdSe quantum dots, Figure 3C), *i.e.*, ~10^5 times slower.

The data here may also have ramifications for understanding the relationships between delayed luminescence and single-quantum-dot blinking proposed in several studies.[1,3-5,8] If it is correct to equate the metastable charge-separated state of delayed luminescence with a blinking "off" state, then the finding that the excitation pulse duration affects the detrapping kinetics should imply a dependence of blinking "off"-time statistics on similar excitation parameters. To our knowledge, there have been no single-quantum-dot blinking studies employing variable pulse-width excitation, however. An early study reported a change in the number of "on"/"off" cycles with different continuous-wave (cw) excitation powers between 0.4 and 7.8 kW/cm^2.[20] Another study varied the cw excitation power density from 0.1 to 2.0 kW/cm^2 and did not see any effect on the "off"-time statistics.[21] A recent study compared pulsed *vs* cw excitation at the same average intensity and found that the main impact of pulsed excitation was to increase

photobleaching.[22] These authors also reported that pulsed excitation lowers the probability of long "on" events, but they do not describe any significant change in "off"-time statistics.[22] As noted recently,[5] one complication in any direct comparison between blinking and delayed luminescence is the fact that only a subset of the traps that contribute to blinking will also generate delayed luminescence. Moreover, it is conceivable that some of the kinetic dispersion observed in the delayed luminescence arises from the quantum dot ensemble and would therefore not be observed from an individual quantum dot, although we note that even single-quantum-dot delayed luminescence shows broadly distributed decay dynamics.[1]

In summary, we report two main observations that have not been described previously: (*i*) quantum-dot delayed luminescence decay dynamics are strongly influenced by the experimental excitation conditions, and (*ii*) such dynamics are particularly sensitive to excitation pulse duration, a parameter that is rarely examined systematically or controlled for experimentally. For both CdSe and $CuInS_2$ quantum dots, decay of the delayed luminescence is strikingly slower when longer excitation pulses are used. Short (*e.g.*, ns) excitation pulses generate markedly less delayed luminescence than long (*e.g.*, μs) excitation pulses, and very long (>ms) excitation pulses are required to reach a regime in which the delayed luminescence no longer depends on the excitation pulse width. Modeling shows that this behavior reflects the extremely long excitation times required for the population of the metastable charge-separated excited states responsible for delayed luminescence to reach steady state, and that the main parameter affecting this approach to steady state is the detrapping rate constant. Although these simulations successfully reproduce the major experimental observations from our excitation pulse-width and power-dependence measurements, our idealized model does not include distributed rate constants and consequently does not reproduce the experimental dependence of N_{del}/N_{pr} on the

delayed luminescence integration window, or the change in average decay rate with changing excitation pulse width, emphasizing the importance of such distributed kinetics. Overall, these findings shed new light on the ubiquitous phenomenon of delayed luminescence in colloidal quantum dots, and hence on the underlying charge-carrier trapping and detrapping processes that so strongly impact the physical properties of this class of materials.

ASSOCIATED CONTENT

Supporting Information. Additional experimental details, absorption and ensemble photoluminescence data, linear plots of delayed luminescence dynamics, comparison of the change in dynamics for changing the excitation power and pulse width by similar factors, normalized plots of power-dependence data, simulated luminescence decay curves, simulated pulse-width dependence of N_{del}/N_{pr} for different integration windows and with different nonradiative processes, and comparison of experimental long-pulse decay curves with decay curves simulated by summing experimental short-pulse decay curves.

AUTHOR INFORMATION

Corresponding Author

***** Department of Chemistry, University of Washington, Seattle, Washington, 98195-1700 USA, E-mail: gamelin@chem.washington.edu, Ph: (206)-685-0901

‡ These authors contributed equally.

Present Addresses

† Department of Chemistry, University of Rochester, Rochester, NY 14627, USA

§ Laboratory for Fundamental BioPhotonics, Institute of Bioengineering and Institute of Materials Science, School of Engineering, École Polytechnique Fédérale de Lausanne (EPFL), CH-1015 Lausanne, Switzerland

ACKNOWLEDGMENT

Financial support from the National Science Foundation (DMR-1505901 to D.R.G. and CHE-1404674 to P.J.R.) is gratefully acknowledged. A. M. acknowledges the support of an Early Postdoc Mobility Fellowship from the Swiss National Science Foundation. K.E.K. thanks the Department of Energy for support through an Energy Efficiency and Renewable Energy (EERE) postdoctoral research award. We thank Dr. Charles Barrows and Mr. Troy Kilburn for synthesis of the CdSe and $CuInS_2$ quantum dot samples used in these studies. Part of this work was conducted at the UW Molecular Analysis Facility, which is supported in part by funds from the UW Molecular Engineering & Sciences Institute, the UW Clean Energy Institute, the National Science Foundation, and the National Institutes of Health.

REFERENCES

(1) Sher, P. H.; Smith, J. M.; Dalgarno, P. A.; Warburton, R. J.; Chen, X.; Dobson, P. J.; Daniels, S. M.; Pickett, N. L.; O'Brien, P. Power Law Carrier Dynamics in Semiconductor Nanocrystals at Nanosecond Timescales. *Appl. Phys. Lett.* **2008**, *92*, 101111.

(2) Jones, M.; Lo, S. S.; Scholes, G. D. Quantitative Modeling of the Role of Surface Traps in CdSe/CdS/ZnS Nanocrystal Photoluminescence Decay Dynamics. *Proc. Nat. Acad. Sci. U. S. A.* **2009**, *106*, 3011-3016.

(3) Whitham, P. J.; Knowles, K. E.; Reid, P. J.; Gamelin, D. R. Photoluminescence Blinking and Reversible Electron Trapping in Copper-Doped CdSe Nanocrystals. *Nano Lett.* **2015**, *15*, 4045-4051.

(4) Rabouw, F. T.; Kamp, M.; van Dijk-Moes, R. J. A.; Gamelin, D. R.; Koenderink, A. F.; Meijerink, A.; Vanmaekelbergh, D. Delayed Exciton Emission and Its Relation to Blinking in CdSe Quantum Dots. *Nano Lett.* **2015**, *15*, 7718-7725.

(5) Marchioro, A.; Whitham, P. J.; Knowles, K. E.; Kilburn, T. B.; Reid, P. J.; Gamelin, D. R. Tunneling in the Delayed Luminescence of Colloidal CdSe, Cu^{+}-Doped CdSe, and $CuInS_2$ Semiconductor Nanocrystals and Relationship to Blinking. *J. Phys. Chem. C* **2016**, *120*, 27040-27049.

(6) Rabouw, F. T.; van der Bok, J. C.; Spinicelli, P.; Mahler, B.; Nasilowski, M.; Pedetti, S.; Dubertret, B.; Vanmaekelbergh, D. Temporary Charge Carrier Separation Dominates the Photoluminescence Decay Dynamics of Colloidal CdSe Nanoplatelets. *Nano Lett.* **2016**, *16*, 2047-2053.

(7) Chirvony, V. S.; González-Carrero, S.; Suarez, I.; Galian, R. E.; Sessolo, M.; Bolink, H. J.; Martinez-Pastor, J. P.; Pérez-Prieto, J. Delayed Luminescence in Lead Halide Perovskite Nanocrystals. *J. Phys. Chem. C* **2017**, *121*, 13381-13390.

(8) Whitham, P. J.; Marchioro, A.; Knowles, K. E.; Kilburn, T. B.; Reid, P. J.; Gamelin, D. R. Single-Particle Photoluminescence Spectra, Blinking, and Delayed Luminescence of Colloidal $CuInS_2$ Nanocrystals. *J. Phys. Chem. C* **2016**, *120*, 17136-17142.

(9) Tachiya, M.; Seki, K. Unified Explanation of the Fluorescence Decay and Blinking Characteristics of Semiconductor Nanocrystals. *Appl. Phys. Lett.* **2009**, *94*, 081104.

(10) Nirmal, M.; Dabbousi, B. O.; Bawendi, M. G.; Macklin, J. J.; Trautman, J. K.; Harris, T. D.; Brus, L. E. Fluorescence Intermittency in Single Cadmium Selenide Nanocrystals. *Nature* **1996**, *383*, 802-804.

(11) Efros, A. L.; Nesbitt, D. J. Origin and Control of Blinking in Quantum Dots. *Nat. Nanotechnol.* **2016**, *11*, 661-671.

(12) Cordones, A. A.; Leone, S. R. Mechanisms for Charge Trapping in Single Semiconductor Nanocrystals Probed by Fluorescence Blinking. *Chem. Soc. Rev.* **2013**, *42*, 3209-3221.

(13) van Schooten, K. J.; Huang, J.; Talapin, D. V.; Boehme, C.; Lupton, J. M. Spin-Dependent Electronic Processes and Long-Lived Spin Coherence of Deep-Level Trap Sites in CdS Nanocrystals. *Phys. Rev. B* **2013**, *87*, 125412.

(14) Jha, P. P.; Guyot-Sionnest, P. Trion Decay in Colloidal Quantum Dots. *ACS Nano* **2009**, *3*, 1011-1015.

(15) Cohn, A. W.; Rinehart, J. D.; Schimpf, A. M.; Weaver, A. L.; Gamelin, D. R. Size Dependence of Negative Trion Auger Recombination in Photodoped CdSe Nanocrystals. *Nano Lett.* **2014**, *14*, 353-358.

(16) Cohn, A. W.; Schimpf, A. M.; Gunthardt, C. E.; Gamelin, D. R. Size-Dependent Trap-Assisted Auger Recombination in Semiconductor Nanocrystals. *Nano Lett.* **2013**, *13*, 1810-1815.
(17) Allan, G.; Delerue, C. Fast Relaxation of Hot Carriers by Impact Ionization in Semiconductor Nanocrystals: Role of Defects. *Phys. Rev. B* **2009**, *79*, 195324.
(18) Sun, J.; Ikezawa, M.; Wang, X.; Jing, P.; Li, H.; Zhao, J.; Masumoto, Y. Photocarrier Recombination Dynamics in Ternary Chalcogenide $CuInS_2$ Quantum Dots. *Phys. Chem. Chem. Phys.* **2015**, *17*, 11981-11989.
(19) Singh, G.; Guericke, M. A.; Song, Q.; Jones, M. A Multipulse Time-Resolved Fluorescence Method for Probing Second-Order Recombination Dynamics in Colloidal Quantum Dots. *J. Phys. Chem. C* **2014**, *118*, 14692-14702.
(20) Banin, U.; Bruchez, M.; Alivisatos, A. P.; Ha, T.; Weiss, S.; Chemla, D. S. Evidence for a Thermal Contribution to Emission Intermittency in Single CdSe/CdS Core/Shell Nanocrystals. *J. Chem. Phys.* **1999**, *110*, 1195-1201.
(21) Shimizu, K. T.; Neuhauser, R. G.; Leatherdale, C. A.; Empedocles, S. A.; Woo, W. K.; Bawendi, M. G. Blinking Statistics in Single Semiconductor Nanocrystal Quantum Dots. *Phys. Rev. B* **2001**, *63*, 205316.
(22) Smyder, J. A.; Amori, A. R.; Odoi, M. Y.; Stern, H. A.; Peterson, J. J.; Krauss, T. D. The Influence of Continuous vs. Pulsed Laser Excitation on Single Quantum Dot Photophysics. *Phys. Chem. Chem. Phys.* **2014**, *16*, 25723-25728.